KSME

Springer

Journal of Mechanical Science and Technology 34 (9) 2020

Original Article
DOI 10.1007/s12206-020-0809-9

Keywords:
· Cable-driven parallel robots
· The cable element
· The finite element method
· The analytical method
· Vibration analysis
· Natural frequencies

Correspondence to:
Kwan-Woong Gwak
kwgwak@sejong.ac.kr

Citation:
Nguyen-Van, S., Gwak, K.-W., Nguyen, D.-H., Lee, S.-G., Kang, B. H. (2020). A novel modified analytical method and finite element method for vibration analysis of cable-driven parallel robots. Journal of Mechanical Science and Technology 34 (9) (2020) 3575~3586. http://doi.org/10.1007/s12206-020-0809-9

Received February 25th, 2020
Revised June 17th, 2020
Accepted July 3rd, 2020

† Recommended by Editor No-cheol Park

A novel modified analytical method and finite element method for vibration analysis of cable-driven parallel robots

Sy Nguyen-Van[1,2], Kwan-Woong Gwak[1], Duc-Hai Nguyen[1], Soon-Geul Lee[3] and Byoung Hun Kang[4]

[1]Department of Mechanical and Aerospace Engineering, Sejong University, 209 Neungdong-Ro, Gwangjin-gu, Seoul 05006, Korea, [2]Faculty of Mechanical Engineering, Thai Nguyen University of Technology, Thai Nguyen, Vietnam, [3]School of Mechanical Engineering, Kyung Hee University, 1732, Deogyeong-daero, Giheung-gu, Yongin-si, Gyeonggi-do 17104, Korea, [4]Department of Mechanical Design Engineering, Korea Polytechnic University, 2121, Jeongwang-dong, Siheung 429-793, Korea

Abstract Cable-driven parallel robots (CDPRs) are vulnerable to vibration due to the inevitable flexible properties of the cables. Thus, vibration analysis is critical for CDPR's operation in which highly accurate motion is required. However, most of the current methods related to vibration analysis of CDPRs rely on simple spring models which have limitations in their performance and complexity that are not general to analyze the vibration of various CDPRs. Hence, accurate, simple and general approaches for vibration analysis in CDPRs are need. To solve this problem, this paper presents the finite element method (FEM) and the modified analytical method to analyze the vibration of CDPRs. To validate these methods, free vibration analysis was conducted using the proposed methods for the planar and spatial cable-driven parallel robots. The natural frequencies of these two CDPRs were computed by the proposed two methods and compared with those of the commercial software, SAP2000. The solutions obtained by the FEM and the modified analytical models turned out to be close to SAP2000's results, thereby verifying the validity of the proposed methods.

1. Introduction

Recently, animal-inspired robots have attracted many researchers [1-5] and a cable-driven parallel robot (called CDPR) is one of them, like a spider with its spiderweb. The CDPR is also a typical type of parallel robot. In CDPR, rigid links are replaced with flexible cables. The end-effector is connected to the supporting frame by a number of cables, and by controlling the cable length, the end-effector can be moved along the desired trajectory [6]. Because of using flexible cables instead of rigid links, the inertia properties of CDPR are automatically much reduced. Hence, the dynamic capability of CDPRs is more advanced than rigid parallel robots [7]. Consequently, as reported in Refs. [8-10], the cutting-edge characteristics of CDPRs are a large workspace, cost saving, lightweight, flexible reconfiguration, and easy transportation.

However, cables used in CDPRs are highly capable of vibration in both axial and transversal directions due to the inevitably flexible characteristics of cables [7] and the performance of CDPRs related to kinematics, positioning accuracy, force distribution, and control depends on their vibration or stiffness [11]. Thus, the vibration and stiffness analysis of CDPRs are more critical than those of the rigid parallel robots. Especially, for CDPRs used for applications requiring highly accurate motion, such as constructional 3D printing [8, 12], pay-loading [13, 14], motion simulation [15], these issues are very important because they provide useful information for dynamic analysis and controller design to enhance the position accuracy along a trajectory.

In the vibration or stiffness analysis for CDPRs, three popular approaches are available: (1) the simplified model of CDPRs based on spring elements, (2) the dynamic stiffness method, and (3) the finite element approach. However, these approaches still have poor accuracy,

complex formulations or limited generality.

For instance, in the case of the first approach, as reported in Ref. [7], the authors modeled cable elements as axial springs and the end-effector as a rigid body to find the natural frequency of a 6-DOF 7-cable manipulator. The same assumptions of cable modeling as linear spring can be found in Refs. [16, 17]. Another method in which modeling the cable as nonlinear springs was also reported in Ref. [18]. However, it could be seen that assuming the cable as a simple spring element for stiffness analysis or determination of the natural frequencies of CDPRs leads to the accuracy problem, because of the highly nonlinear and flexible characteristic and the sagging effects of cable elements.

To overcome this problem, Yuan et al. [19] proposed the dynamic stiffness method to find the static stiffness and the dynamic stiffness for a 6-DOF suspended CDPR driven by eight cables. However, considering the elasticity of pulleys and the end-effector, the dynamic stiffness method was not suited either. Additionally, only one element was used for each cable to derive the cable stiffness; thus it was not possible to get a dynamic response for some arbitrary internal nodes along each cable.

The finite element approach is one of the most frequently used methods to analyze vibration, but it is not the case with the vibration analysis for CDPRs and only several works have been reported. Du et al. [20] proposed a finite difference approximation to solve the dynamic model of CDPRs in which it considers the relation between the motion of the end-effector and the cable force. However, the computational time is relatively expensive for its nonlinear dynamic equation. Do and Park [21] also used a finite element method for CDPRs, but they did not provide a general mathematical model of CDPRs. They only used the element Link 10 in ANSYS to model the cable element of CDPRs.

To overcome the above limitations, this paper presents a new finite element formulation for the cables for the vibration analysis of CDPRs. Originally, this cable formulation was developed in Refs. [22, 23] for constructional structures, but in this research this formulation is first investigated for CDPRs. The advantage of this finite element model is that it provides simple, general and accurate models for vibration analysis of CDPRs because the cable element can be considered as an equivalent truss element for easy computation and the effect of initial tension is also included in the stiffness of cables.

The exact analytical approach is another popular method used for vibration analysis in constructional structures [24-26] because it can present the realistic vibrational behavior of cables. However, there have been no researches using this approach for the vibration analysis for CDPRs. Thus, this paper also presents the vibration analysis of CDPRs using the analytical expression. One of the most considerable works in modeling the cable by the analytical approach is the one used in Ref. [26]. However, this analytical formulation still has two limitations. Because this formulation used only a single two-node element for each cable, it is impossible to get the vibration

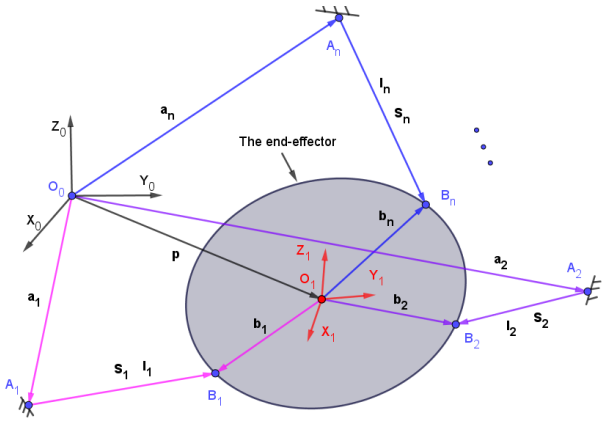

Fig. 1. A general scheme of cable robots [27].

behaviors of internal nodes. Additionally, in the iteration loop of the Newton-Raphson method, the stopping criterion is the error of the projected lengths of cables; thus perfectly vertical cables cannot be modeled. To overcome these shortcomings, a modified procedure of the analytical formulation for calculating the stiffness of CDPRs is proposed in this research to model both internal nodes of cables and perfectly vertical cables. For this objective, each cable is divided into a number of elements and the stiffness matrix of each element is directly calculated without Newton-Raphson iteration.

To validate the feasibility of the FEM and the modified analytical approach proposed in this research, those methods were applied to a generalized planar CDPR model and a spatial CDPR model. The models of CDPRs are built by MATLAB codes. Natural frequencies of CDPRs are computed and compared with those from a commercial software, SAP2000. The main advantage of using the two proposed methods compared with the use of SAP2000 is time-saving in developing various models of CDPRs and they provide general formulations of cables for modeling of CDPRs which SAP2000 cannot.

2. Kinematics and tension distribution of cable-driven parallel robots

Let us consider a general scheme of CDPRs driven by n cables as shown in Fig. 1. The i^{th} cable is attached on the base and the end effector at A_i and B_i, respectively. The vector $\mathbf{l}_i$ denotes the i^{th} cable and its norm is the length of the cable. $\mathbf{S}_i$ is the unit vector of the i^{th} cable. With the global frame O_0, the positions of A_i and the centroid of the end effector (the point O_1) are vectors $\mathbf{a}_i$ and $\mathbf{p}$, respectively. The reference frame is attached at point O_1 and $\mathbf{b}_i$ is the position vector of the point B_i [27].

$$\mathbf{p} = \mathbf{a}_i + \mathbf{l}_i - \mathbf{b}_i \qquad (i = 1, 2, ..., n) \tag{1}$$

where all the vectors are measured with respect to the global frame, O_0.

From Eq. (1), we have the first equation of the kinematics as follows:

$$\mathbf{l}_i^2=\left[\mathbf{p}-\mathbf{a}_i+\mathbf{b}_i\right]^T\left[\mathbf{p}-\mathbf{a}_i+\mathbf{b}_i\right]. \tag{2}$$

Next, we differentiate the above equation with respect to time and then organize the *n* equations into a matrix form as follows:

$$\dot{\mathbf{L}}=\mathbf{Jt} \tag{3}$$

where

$$\dot{\mathbf{L}}=[\dot{l}_1 \quad \dot{l}_2 \quad \ldots \quad \dot{l}_n]^T \tag{4}$$

$$\mathbf{J}=\begin{bmatrix}\mathbf{S}_1 & \mathbf{S}_2 & \ldots & \mathbf{S}_n\\ \mathbf{b}_1\times\mathbf{S}_1 & \mathbf{b}_2\times\mathbf{S}_2 & \ldots & \mathbf{b}_n\times\mathbf{S}_n\end{bmatrix}^T \tag{5}$$

$$\mathbf{t}=\begin{bmatrix}\dot{\mathbf{p}}^T\\ \boldsymbol{\omega}^T\end{bmatrix} \tag{6}$$

where $\dot{\mathbf{p}}$ and $\boldsymbol{\omega}$ are the linear velocity vector of point O_1 and the angular velocity vector of the end effector, respectively; **J** is the *n x 6* Jacobian matrix of the cable robot.

Let $\mathbf{T}=[T_1 \quad T_2 \quad \ldots \quad T_n]^T$ be the vector of cable forces. In CDPRs, cables cannot be compressed and the applied cable forces must satisfy the force closure condition [28]. Thus, the vector of cable forces **T** can be generated as follows:

$$\mathbf{J}^T\mathbf{T}=\mathbf{w} \tag{7}$$

where **w** is the resultant wrench applied at the end effector and is given as follows:

$$\mathbf{w}=\begin{bmatrix}-m\mathbf{g}\\ \mathbf{0}_{3\times1}\end{bmatrix}+\begin{bmatrix}\mathbf{f}_e\\ \boldsymbol{\tau}_e\end{bmatrix} \tag{8}$$

where *m* is the mass of the end effector; **g** is the gravitational acceleration vector; $\mathbf{f}_e$ and $\boldsymbol{\tau}_e$ the external force vector and the external moment vector applied to the end-effector, respectively.

As reported in Ref. [28], to calculate the tension applied to cables, there is a need for the tension distribution algorithm to handle the over-constraint condition and nonnegativity requirement of the cable. One of the possible approaches is the quadratic or nonlinear programming algorithm, which can be formulated as follows:

$$\text{minimize:}\frac{1}{2}\mathbf{T}^T\mathbf{C}\mathbf{T}+\mathbf{c}^T\mathbf{T} \tag{9}$$

$$\text{subject to:}T_{\min}\le T_i\le T_{\max} \tag{10}$$

$$\mathbf{J}^T\mathbf{T}=\mathbf{w} \tag{11}$$

where **C** and **c** are the weighting factor for the objective function and T_{max} and T_{min} are the minimum and the maximum tension allowed to cables, respectively. As reported in Ref. [28], due to discontinuities by using the 1-norm as objective function, the 2-norm in the objective function for the quadratic programming is used. Thus, the weighting factors are set as follows: **C = I** for the quadratic part in **T** and **c = 0** for nullifying the linear part.

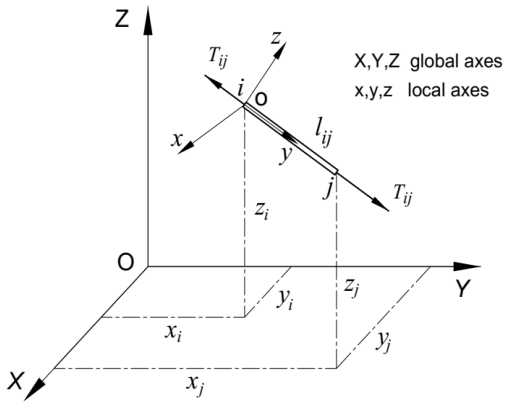

Fig. 2. The equivalent cable-truss element.

3. Formulation problems

For vibration analysis of CDPRs, the finite element method is first presented. Then, a modified analytical approach is proposed to model both perfectly vertical cables and internal nodes of cables.

3.1 Finite element formulation

In this section, the finite element formulation for cable elements is carried out. The cable element is assumed to have two nodes, *i* and *j*, the length, l_{ij} and the applied tension, T_{ij}, as shown in Fig. 2. Then the general equation of motion of cable element is as given follows [23]:

$$\mathbf{M}\ddot{\mathbf{u}}+(\mathbf{K}_L+\mathbf{K}_G)\mathbf{u}=\mathbf{0} \tag{12}$$

where $\ddot{\mathbf{u}}$ and $\mathbf{u}$ are the acceleration and displacement vector, respectively; $\mathbf{K}_L$ is the conventional stiffness matrix; $\mathbf{K}_G$ is the geometric stiffness matrix.

Additionally,

$$\mathbf{u}=\left[u_{xi} \quad u_{yi} \quad u_{zi} \quad u_{xj} \quad u_{yj} \quad u_{zj}\right]^T \tag{13a}$$

$$\mathbf{K}_L=\int_0^1(k_s-T_{ij})l_{ij}\left(\mathbf{N}'^T\mathbf{N}'\boldsymbol{\Delta}\boldsymbol{\Delta}^T\mathbf{N}'^T\mathbf{N}'\right)d\xi \tag{13b}$$

$$\mathbf{K}_G=\int_0^1 T_{ij}l_{ij}\mathbf{N}'d\xi \tag{13c}$$

$$\boldsymbol{\Delta}=\left[x_i \quad y_i \quad z_i \quad x_j \quad y_j \quad z_j\right]^T \tag{13d}$$

where $\mathbf{N}$ is the shape function in the displacement field; $\mathbf{N}'$ is the ordinary differentiation of $\mathbf{N}$; k_s is the elastic stiffness with

$k_s = EA$ and $\zeta = x / l_{ij}$ has a value from 0 to 1 and $\mathbf{\Lambda}$ is the node coordinate vector.

The shape function and its differentiation are given as follows:

$$\mathbf{N} = \left[(1-\xi)\mathbf{I} \quad \xi\mathbf{I}\right]; \mathbf{N}' = \frac{1}{l_{ij}}\left[-\mathbf{I} \quad \mathbf{I}\right]. \tag{14}$$

With **I** being the 3x3 unit matrix, we also have:

$$\mathbf{N}'^{T}\mathbf{N}' = \frac{1}{l_{ij}^2}\begin{bmatrix} \mathbf{I} & -\mathbf{I} \\ -\mathbf{I} & \mathbf{I} \end{bmatrix}. \tag{15}$$

The mass matrix **M** is given as follows:

$$\mathbf{M} = \frac{\gamma l_{ij}}{6g}\begin{bmatrix} 2\mathbf{I} & \mathbf{I} \\ \mathbf{I} & 2\mathbf{I} \end{bmatrix} \tag{16}$$

where γ is the weight per unit length. Then, the stiffness matrix is given as follows:

$$\mathbf{K}_L = \frac{k_s - T_{ij}}{l_{ij}}\begin{bmatrix} \mathbf{G} & -\mathbf{G} \\ -\mathbf{G} & \mathbf{G} \end{bmatrix} \tag{17a}$$

$$\mathbf{K}_G = \frac{T_{ij}}{l_{ij}}\begin{bmatrix} \mathbf{I} & -\mathbf{I} \\ -\mathbf{I} & \mathbf{I} \end{bmatrix} \tag{17b}$$

where **G** is the transformation matrix which transforms the element stiffness matrix of each cable in the local frame (oxy) to the global frame (OXY) and is given as follows:

$$\mathbf{G} = \begin{bmatrix} l^2 & ml & nl \\ ml & m^2 & nm \\ nl & nm & n^2 \end{bmatrix} \tag{18a}$$

$$l = (x_j - x_i)/l_{ij}; m = (y_j - y_i)/l_{ij}; n = (z_j - z_i)/l_{ij}. \tag{18b}$$

3.2 The modified analytical method

This section presents a modified formulation of the analytical approach of cables in the work of Tai and Kim [26]. The two main modifications are that there is no iteration loop of the Newton Raphson method, and the cables are divided into numbers of finite elements. Thus the modified analytical formulation can handle perfectly vertical cables and internal nodes of cables.

A cable element is shown as in Fig. 3. The cable element has two nodes, *I(0,0,0)* and *J*(l_x, l_y, l_z). The undeformed and deformed configurations of the cable element are *s* and *p*, respectively. The three equilibrium equations of the cable element are as follows:

$$T\left(\frac{dx}{dp}\right) = -F_1 \tag{19a}$$

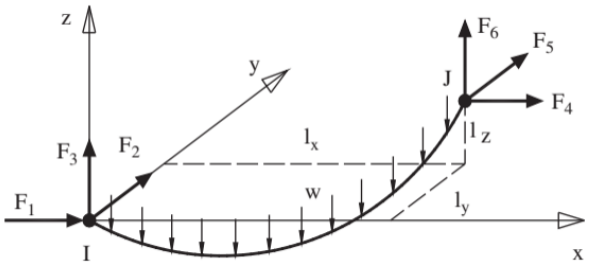

Fig. 3. The three-dimensional catenary cable element [26].

$$T\left(\frac{dy}{dp}\right) = -F_2 \tag{19b}$$

$$T\left(\frac{dz}{dp}\right) = -F_3 + \gamma s \tag{19c}$$

where F_1, F_2, F_3 are the projected components of cable tension in *x*-, *y*-and *z*-axis, respectively; the weight per unit length of the cable is γ; *T* is the applied tension at the Lagrange coordinate *s* and for the case of CDPRs, *T* is calculated from the above-mentioned tension distribution algorithm. The relationship between *T* and the projected tension is given as follows:

$$T(s) = \sqrt{F_1^2 + F_2^2 + (F_3 - \gamma s)^2}. \tag{20}$$

For the cable element, the relationship between tension (*T*) and the strain (ε) is represented by Hooke's law [29] as follows:

$$T = EA\varepsilon = EA\left(\frac{dp - ds}{ds}\right) = EA\left(\frac{dp}{ds} - 1\right) \tag{21}$$

where *E* and *A* are Young's modulus and cross-sectional area of the cable element, respectively.

The Lagrange coordinate *s* and the Cartesian coordinate are related as follows:

$$x = \int_0^L \frac{dx}{ds}ds = \int_0^L \frac{dx}{dp}\frac{dp}{ds}ds \tag{22a}$$

$$y = \int_0^L \frac{dy}{ds}ds = \int_0^L \frac{dy}{dp}\frac{dp}{ds}ds \tag{22b}$$

$$z = \int_0^L \frac{dz}{ds}ds = \int_0^L \frac{dz}{dp}\frac{dp}{ds}ds. \tag{22c}$$

As shown in Fig. 3, six boundary conditions are given as follows:

$$x(0) = y(0) = z(0) \tag{23a}$$

$$x(L_0) = l_x, y(L_0) = l_y, z(L_0) = l_z. \tag{23b}$$

Now, substituting Eqs. (19)-(21) into Eq. (22), we have the three equations of the projected lengths of the cable are as follows:

$$l_x = -\frac{F_1 L_0}{EA} - \frac{F_1}{\gamma}\{\ln\left[\sqrt{F_1^2 + F_2^2 + \left(-F_3 + \gamma L_0\right)^2}\right] + \\ + \gamma L_0 - F_0 - \ln\left(\sqrt{F_1^2 + F_2^2 + F_3^2} - F_3\right)\} \tag{24a}$$

$$l_y = -\frac{F_2 L_0}{EA} - \frac{F_2}{\gamma}\{\ln\left[\sqrt{F_1^2 + F_2^2 + \left(-F_3 + \gamma L_0\right)^2}\right] + \\ + \gamma L_0 - F_0 - \ln\left(\sqrt{F_1^2 + F_2^2 + F_3^2} - F_3\right)\} \tag{24b}$$

$$l_z = -\frac{F_3 L_0}{EA} + \frac{\gamma L_0^2}{2EA} + \\ + \frac{1}{\gamma}\left[\sqrt{F_1^2 + F_2^2 + \left(-F_3 + \gamma L_0\right)^2} - \sqrt{F_1^2 + F_2^2 + F_3^2}\right] \tag{24c}$$

where L_0 is the unstressed length of the cable. Now, these equations can be written in terms of the node forces (F_1, F_2, F_3):

$$l_x = f\left(F_1, F_2, F_3\right) \tag{25a}$$

$$l_y = g\left(F_1, F_2, F_3\right) \tag{25b}$$

$$l_z = h\left(F_1, F_2, F_3\right). \tag{25c}$$

Differentiating these above equations with respect to F_1, F_2, F_3, we have:

$$dl_x = \frac{\partial f}{\partial F_1} dF_1 + \frac{\partial f}{\partial F_2} dF_2 + \frac{\partial f}{\partial F_3} dF_3 \tag{26a}$$

$$dl_y = \frac{\partial g}{\partial F_1} dF_1 + \frac{\partial g}{\partial F_2} dF_2 + \frac{\partial g}{\partial F_3} dF_3 \tag{26b}$$

$$dl_z = \frac{\partial h}{\partial F_1} dF_1 + \frac{\partial h}{\partial F_2} dF_2 + \frac{\partial h}{\partial F_3} dF_3 . \tag{26c}$$

Writing into a matrix form, we can get:

$$\begin{bmatrix} dl_x \\ dl_y \\ dl_z \end{bmatrix} = \begin{bmatrix} f_{11} & f_{12} & f_{13} \\ f_{21} & f_{22} & f_{23} \\ f_{31} & f_{32} & f_{33} \end{bmatrix} \begin{bmatrix} dF_1 \\ dF_2 \\ dF_3 \end{bmatrix} = F \begin{bmatrix} dF_1 \\ dF_2 \\ dF_3 \end{bmatrix} \tag{27}$$

where F is the flexibility matrix and the equations of elements are given as follows:

$$f_{11} = -\left(\frac{L_0}{EA} + \frac{1}{\gamma}\log\frac{T_j + F_6}{T_i - F_3}\right) + \\ + \frac{F_1^2}{\gamma}\left[\frac{1}{T_i\left(T_i - F_3\right)} - \frac{1}{T_j\left(T_j + F_6\right)}\right] \tag{28a}$$

$$f_{12} = f_{21} = \frac{F_1 F_2}{\gamma}\left[\frac{1}{T_i\left(T_i - F_3\right)} - \frac{1}{T_j\left(T_j + F_6\right)}\right] \\ f_{13} = f_{31} = \frac{F_1}{\gamma}\left[\frac{1}{T_j} - \frac{1}{T_i}\right] \tag{28b}$$

$$f_{22} = -\left(\frac{L_0}{EA} + \frac{1}{\gamma}\log\frac{T_j + F_6}{T_i - F_3}\right) + \\ + \frac{F_2^2}{\gamma}\left[\frac{1}{T_i\left(T_i - F_3\right)} - \frac{1}{T_j\left(T_j + F_6\right)}\right] \tag{28c}$$

$$f_{23} = f_{32} = \frac{F_2}{\gamma}\left[\frac{1}{T_i} - \frac{1}{T_j}\right] \\ f_{33} = -\frac{L_0}{EA} - \frac{1}{\gamma}\left[\frac{F_6}{T_j} + \frac{F_3}{T_i}\right]. \tag{28d}$$

With, T_i and T_j are initial tensions applied to cable robots:

$$T_i = \sqrt{F_1^2 + F_2^2 + F_3^2} \tag{29a}$$

$$T_j = \sqrt{F_4^2 + F_5^2 + F_6^2} \tag{29b}$$

where

$$F_4 = -F_1 \tag{30a}$$

$$F_5 = -F_2 \tag{30b}$$

$$F_6 = -F_3 + \gamma L_0 . \tag{30c}$$

So, finally, the stiffness matrix is given as follows:

$$\mathbf{K} = \mathbf{F}^{-1} = \begin{bmatrix} f_{11} & f_{12} & f_{13} \\ f_{21} & f_{22} & f_{23} \\ f_{31} & f_{32} & f_{33} \end{bmatrix}^{-1} . \tag{31}$$

The tangent stiffness matrix is given as follows:

$$\mathbf{K}_T = \begin{bmatrix} -\mathbf{K} & \mathbf{K} \\ \mathbf{K} & -\mathbf{K} \end{bmatrix}. \tag{32}$$

For CDPRs, applied cable tensions (T_0) in the modified analytical formulation are generated by tension distribution algorithm in Sec. 2. Then, the modified procedure for calculation of the stiffness matrix of cables can be given as follows:

Step 1: input *w, E, A* and nodes $I(x_i, y_i, z_i)$, $J(x_j, y_j, z_j)$.

Step 2: calculate $l_{x0} = x_j - x_i, l_{y0} = y_j - y_i, l_{z0} = z_j - z_i$.

Step 3: initialization the values of L_0, F_1, F_2, F_3.

$$L_0 = \sqrt{l_{x0}^2 + l_{y0}^2 + l_{z0}^2}$$

$$F_1 = -\frac{l_{x0}}{L_0} T_0$$

$$F_2 = -\frac{l_{y0}}{L_0} T_0$$

$$F_3 = -\frac{l_{z0}}{L_0} T_0 .$$

Step 4: calculate T_i and T_j using Eqs. (29a) and (29b).

Table 1. The dimensions of the planar CDPR.

Position vector	x (m)	y (m)	Position vector	x (m)	y (m)
A_1	1.25	1.25	A_3	-1.25	-1.25
A_2	-1.25	1.25	A_4	1.25	-1.25

Table 2. Data for the free vibration problem of the planar CDPR [30].

Parameters (unit)	Value
The cross-sectional areas $A(\mathrm{m}^2)$	12.56×10^{-6}
The mass of the end effector (kg)	5
The modulus of elasticity $E(\mathrm{N/m}^2)$	2.0×10^{10}
The weight per unit length $\gamma(\mathrm{N/m})$	0.067
The minimum tension $T_{min}(\mathrm{N})$	$[20,40,60,80]$
The maximum tension $T_{max}(\mathrm{N})$	250

Step 5: calculate the stiffness matrix by Eqs. (31) and (32).

In this modified procedure, there is no Newton-Raphson iteration for updating the misclosure vector: $dL = \{(l_{xo}-l_x)\ \ (l_{yo}-l_y)\ \ (l_{zo}-l_z)\}^T$. Thus, this algorithm can model perfectly vertical cables.

4. Natural frequencies of CDPRs

To evaluate the stiffness or dynamic performance of CDPRs, the natural frequency obtained from free vibration analysis is a good parameter.

Regarding the free vibration analysis of CDPRs, the following assumptions are made:

1) The mass of the end effector is a point mass attached at the centroid of the end effector.

2) All cables are connected at the centroid of the end effector.

3) Friction in gearbox and pulleys in CDPRs are neglected.

4) Cable materials are isotropic.

5) Applied tension for cables are calculated by a tension distribution algorithm solved by the quadratic programming as mentioned in Sec. 2.

For the free vibration problem of CDPRs, the general equation of motion of CDPRs' structure is given as follows:

$$\mathbf{M}\ddot{\mathbf{u}} + \mathbf{K}\mathbf{u} = \mathbf{0} \tag{33}$$

where **M** and **K** are the global mass matrix and the global stiffness matrix, respectively.

The eigenvalue problem is given as follows:

$$\left(\mathbf{M} - \omega^2\mathbf{K}\right)\bar{\mathbf{u}} = \mathbf{0} \tag{34}$$

where ω and $\bar{\mathbf{u}}$ are the natural frequency of cable robots and the associated displacement vector. To get the nontrivial solutions of the eigenvalue problem, the following determinant must be equal to zero:

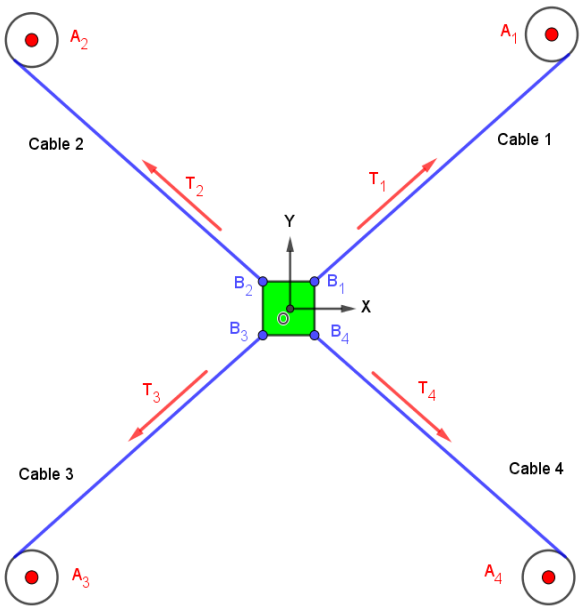

Fig. 4. A generalized planar cable driven parallel robot.

$$\left|\mathbf{M} - \omega^2\mathbf{K}\right| = \mathbf{0}. \tag{35}$$

4.1 A planar cable-driven parallel robot

To validate the performance of the proposed methods to analyze the vibration of CDPRs, a generalized planar CDPR as shown in Fig. 4 is considered first.

First, the planar CDPR is assumed to locate at the position $x = 0$ and $y = 0$, then the dimension of the planar CDPR and the data for the free vibration analysis are summarized in Tables 1 and 2.

Table 3 shows the first ten natural frequencies from the vibration analysis using the FEM model in terms of numbers of elements when the minimum tension T_{min} was set to 20 N. The number of elements was tried up to 40. With the same numbers of elements (40 elements) for each cable in SAP 2000 model, it is apparent that the ten natural frequencies obtained from the FEM model are close to that of SAP2000 with minimum and maximum errors of 1.52 % and 2.13 %, respectively.

Fig. 5 shows the convergence rate of the finite element algorithm for the natural frequency of third mode in Table 3, and it is seen that it converges quickly after six elements. It is also shown that the natural frequencies converge to the 15.39 Hz and 30.29 Hz for the modes between the second and tenth, respectively. It proves that the required number of elements in CDPRs' models is relatively small and as a result, time-consumption is not expensive.

The modified analytical formulation proposed for CDPRs is now applied and Table 4 shows the comparison of the natural frequencies obtained by the modified analytical model, the FEM model and SAP2000 for four different lower-boundary values of cable forces, T_{min}. In all three models, each cable is

Table 3. The natural frequencies (Hz) of the first ten modes for a planar CDPR with T_{min} = 20 N.

No. of elements	Mode									
	1	2	3	4	5	6	7	8	9	10
1	0.48	38.10	38.10	0.00	0.00	0.00	0.00	0.00	0.00	0.00
2	0.48	16.96	16.96	16.97	16.97	16.97	16.97	16.97	16.98	38.12
4	0.48	15.78	15.78	15.79	15.79	15.79	15.79	15.79	15.80	33.92
6	0.48	15.56	15.56	15.56	15.56	15.56	15.56	15.56	15.58	32.18
8	0.48	15.48	15.48	15.49	15.49	15.49	15.49	15.49	15.50	31.56
10	0.48	15.45	15.45	15.45	15.45	15.45	15.45	15.45	15.47	31.27
20	0.48	15.40	15.40	15.40	15.40	15.40	15.40	15.40	15.42	30.89
40	0.48	15.39	15.39	15.39	15.39	15.39	15.39	15.39	15.41	30.80
SAP2000	0.47	15.16	15.16	15.16	15.16	15.16	15.16	15.16	15.17	30.29
Error	2.13%	1.52%	1.52%	1.52%	1.52%	1.52%	1.52%	1.52%	1.58%	1.68%

Table 4. Comparison of the natural frequency for a planar cable-driven parallel robot.

T_{min}	20 N			40 N			60 N			80 N		
Mode	Frequency (Hz)			Frequency (Hz)			Frequency (Hz)			Frequency (Hz)		
	SAP2000	By Matlab		SAP2000	By Matlab		SAP2000	By Matlab		SAP2000	By Matlab	
		Analytical	FEM		Analytical	FEM		Analytical	FEM		Analytical	FEM
1	0.474	0.481	0.481	0.675	0.680	0.680	0.828	0.832	0.832	0.956	0.961	0.961
2	15.157	15.448	15.449	21.608	21.843	21.845	26.481	26.745	26.748	30.571	30.867	30.872
3	15.157	15.449	15.449	21.608	21.843	21.845	26.481	26.745	26.748	30.571	30.867	30.872
4	15.159	15.450	15.450	21.613	21.849	21.850	26.493	26.758	26.761	30.599	30.896	30.901
5	15.159	15.450	15.450	21.613	21.849	21.850	26.493	26.758	26.761	30.599	30.896	30.901
6	15.159	15.450	15.450	21.613	21.849	21.850	26.493	26.758	26.761	30.599	30.896	30.901
7	15.159	15.450	15.451	21.613	21.849	21.850	26.493	26.758	26.761	30.599	30.896	30.901
8	15.159	15.450	15.451	21.613	21.849	21.851	26.493	26.758	26.761	30.599	30.896	30.901
9	15.174	15.465	15.466	21.634	21.870	21.872	26.519	26.784	26.787	30.629	30.926	30.931
10	30.288	31.274	31.275	37.909	38.109	38.110	37.932	38.130	38.130	37.954	38.151	38.151
Mean error	-	0.291	0.292	-	0.236	0.237	-	0.265	0.268	-	0.297	0.302
Computation time (s)	1.0	0.38	0.41	-	-	-	-	-	-	-	-	-

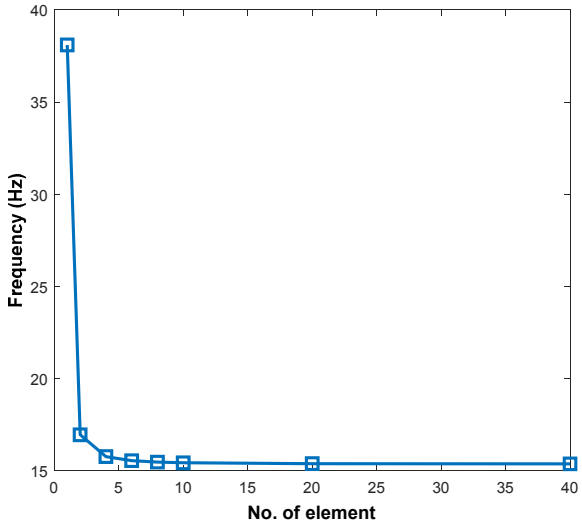

Fig. 5. Convergence rate of natural frequency for mode 3 in Table 3.

divided into 40 elements. It is apparent that results obtained by the FEM and the modified analytical method are almost identical and are very close to those of SAP2000, and the minimum and maximum values of mean errors of 10 modes are 0.236 and 0.302, respectively.

Although these three methods can generate the same results, the time consumption with SAP2000 is considerable in modeling the various CDPRs. Besides, SAP2000 does not provide general formulations of cables and it is difficult to investigate more detailed information. In contrast, the proposed methods are specifically designed for CDPRs. They are simple and easy to modify for other comprehensive CDPR models.

Fig. 6 shows the relationship between the fundamental natural frequency of the CDPR on the values of T_{min}. As shown, when T_{min} increases from 20 N to 60 N, the first natural frequency also increases from 0.48 Hz to 0.96 Hz almost linearly by which dependence of the first natural frequency of the CDPR on the T_{min} is verified. From this observation, it could be

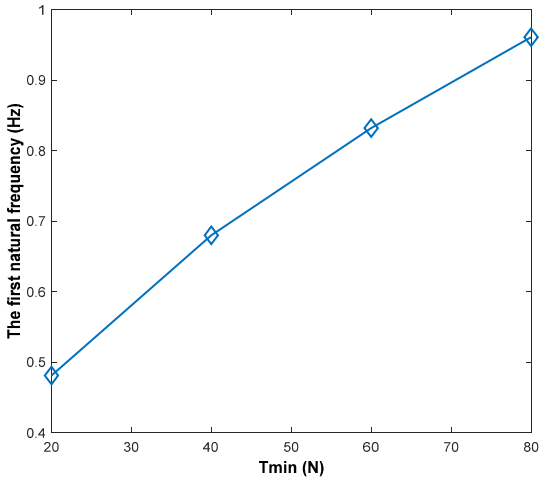

Fig. 6. The dependency of the first natural frequency on T_{min}.

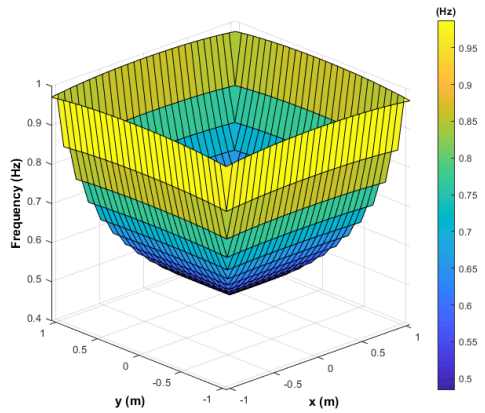

(a)

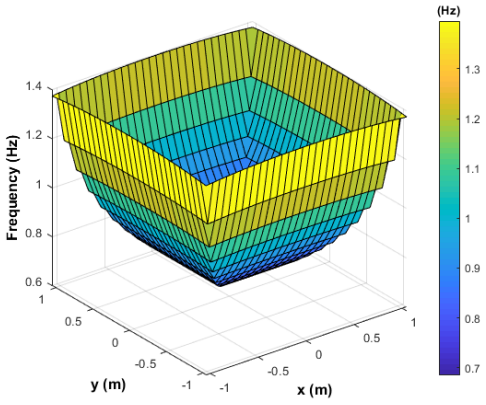

(b)

Fig. 7. The first natural frequency of the planar cable robot in a sub-workspace (-1 m ≤ x ≤ 1 m, -1 m ≤ y ≤ 1 m): (a) T_{min} = 10 N; (b) T_{min} = 40 N.

inferred that the stiffness of CDPRs and the vibration phenomenon can be improved by increasing the value of T_{min} because the stiffness of a structure is related to the natural frequency.

Figs. 7(a) and (b) show the first natural frequency of the planar CDPR in a sub-workspace with two different values of T_{min} = 10 N and 40 N. It is apparent that at the center of the sub-workspace in both figures, the CDPR has the lowest first natural frequency, about 0.481 Hz and 0.68 Hz, respectively. And the first natural frequency is seen to increase as the end-effector goes towards the boundaries of the workspace. The first natural frequency reaches the highest frequency of 0.99 Hz and 1.4 Hz, respectively, at the midpoints of four edges of the workspace. From this first natural frequency distribution results, it can be inferred that for a planar type of CDPR, the cable structure is least stiff and vulnerable to the vibration when the end-effector is positioned at the center of the workspace. In contrast, the planar CDPR has the maximum structural stiffness when the end-effector is located at the midpoints of four top edges in the workspace hence is more robust to the vibration.

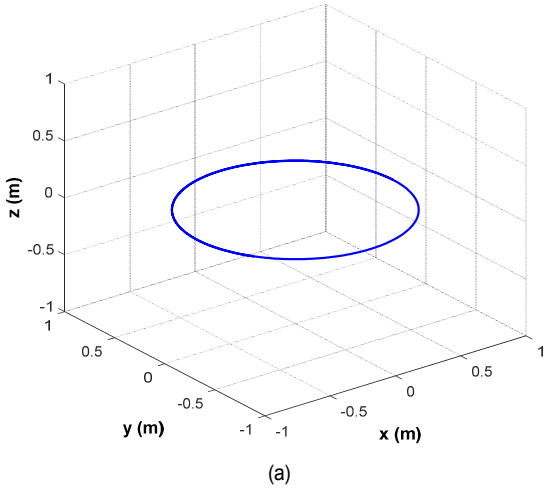

(a)

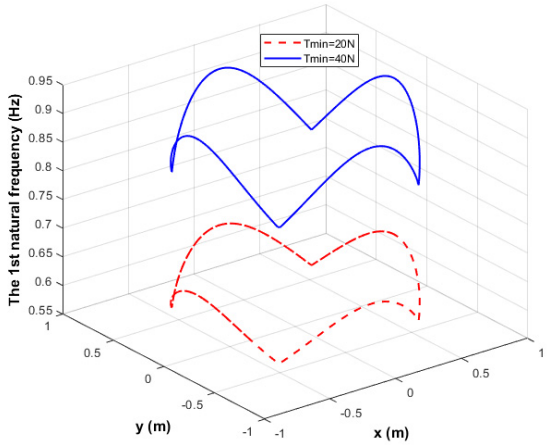

(b)

Fig. 8. (a) The circular trajectory; (b) the first natural frequency of the planar CDPR along the circular trajectory.

Fig. 8(a) shows the circular trajectory for the planar CDPR with a radius of 0.75 m, and Fig. 8(b) illustrates the first natural frequency of CDPRs along the circular trajectory for two different values of T_{min} = 20 N and 40 N. As shown, in the case of

Table 5. The dimensions of the spatial CDPR.

Position vector	x (m)	y (m)	z (m)	Position vector	x (m)	y (m)	z (m)
A_1	1.25	1.25	2.5	A_5	1.25	1.25	0
A_2	-1.25	1.25	2.5	A_6	-1.25	1.25	0
A_3	-1.25	-1.25	2.5	A_7	-1.25	-1.25	0
A_4	1.25	-1.25	2.5	A_8	1.25	-1.25	0

Table 6. Data for the free vibration problem of a spatial cable-driven parallel robot.

Parameters (unit)	Value
Mass of the end effector (kg)	30
The cross-sectional areas A (m^2)	50.265×10^{-6}
The dimensional lengths of the robot's frame (m)	$2.5\times2.5\times2.5$
The position of the end effector, [x,y,z] (m)	[0;0;1.25]
The modulus of elasticity E (N/m^2)	2.01×10^{10}
The weight per unit length γ (N/m)	0.251
The minimum tension T_{min} (N)	[60,80,100,120]
The maximum tension T_{max} (N)	350

Table 7. The natural frequencies (Hz) of the first ten modes for the spatial cable-driven parallel robot obtained by FEM with T_{min} = 60 N.

No. of elements	Mode									
	1	2	3	4	5	6	7	8	9	10
1	32.511	32.511	32.511	0.000	0.000	0.000	0.000	0.000	0.000	0.000
2	12.396	12.396	12.396	12.397	12.397	12.397	12.397	12.397	20.286	20.287
4	11.533	11.533	11.533	11.533	11.533	11.533	11.533	11.533	18.873	18.875
6	11.371	11.371	11.371	11.372	11.372	11.372	11.372	11.372	18.609	18.610
8	11.314	11.314	11.314	11.315	11.315	11.315	11.315	11.315	18.516	18.517
10	11.288	11.288	11.288	11.289	11.289	11.289	11.289	11.289	18.474	18.475
20	11.254	11.254	11.254	11.254	11.254	11.254	11.254	11.254	18.417	18.418
40	11.245	11.245	11.245	11.246	11.246	11.246	11.246	11.246	18.403	18.404
SAP2000	10.978	10.978	10.978	10.978	10.978	10.978	10.978	10.978	18.267	18.269
Error	2.44 %	2.44 %	2.43 %	2.44 %	2.44 %	2.44 %	2.44 %	2.44 %	0.74 %	0.74 %

T_{min} = 40 N, the CDPR cable structure always has higher natural frequencies than those in the case of T_{min} = 20 N. It implies that the stiffness of CDPRs and the vibration resistance can be improved by increasing the value of T_{min}.

4.2 A spatial cable-driven parallel robot

Now the FEM and a modified analytical method are applied to a spatial CDPR driven by eight cables as shown in Fig. 9. Data for the free vibration analysis of the spatial CDPR are summarized in Tables 5 and 6.

Table 7 shows the natural frequencies of the first ten modes of the spatial CDPR using the FEM model with T_{min} set to 60 N. With the same number of elements (40 elements) for each cable in SAP 2000 model, it can see that the ten natural frequencies obtained from the FEM model are close to that of

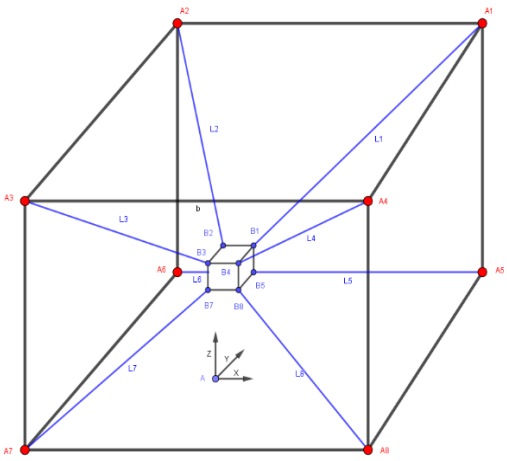

Fig. 9. A spatial cable-driven parallel robot.

Table 8. Comparison of the natural frequency for the spatial cable-driven parallel robot.

T_{min}	60 N			80 N			100 N			120 N		
Mode	Frequency (Hz)			Frequency (Hz)			Frequency (Hz)			Frequency (Hz)		
	SAP2000	By Matlab		SAP2000	By Matlab		SAP2000	By Matlab		SAP2000	By Matlab	
		Analytical	FEM		Analytical	FEM		Analytical	FEM		Analytical	FEM
1	10.978	11.245	11.245	12.815	12.984	12.984	14.382	14.516	14.516	15.780	15.901	15.901
2	10.978	11.245	11.245	12.815	12.984	12.984	14.382	14.516	14.516	15.780	15.901	15.901
3	10.978	11.245	11.245	12.815	12.984	12.984	14.382	14.516	14.516	15.780	15.901	15.901
4	10.978	11.246	11.246	12.817	12.985	12.985	14.384	14.518	14.518	15.782	15.903	15.904
5	10.978	11.246	11.246	12.817	12.985	12.985	14.384	14.518	14.518	15.782	15.903	15.904
6	10.978	11.246	11.246	12.817	12.985	12.985	14.384	14.518	14.518	15.782	15.903	15.904
7	10.978	11.246	11.246	12.817	12.985	12.985	14.384	14.518	14.518	15.782	15.903	15.904
8	10.978	11.246	11.246	12.817	12.985	12.985	14.384	14.518	14.518	15.782	15.903	15.904
9	18.267	18.401	18.403	17.637	17.771	17.773	18.315	18.449	18.451	20.335	20.472	20.474
10	18.269	18.402	18.404	17.638	17.772	17.774	18.316	18.450	18.452	20.337	20.473	20.476
Mean error	-	0.268	0.268	-	0.168	0.168	-	0.134	0.134	-	0.121	0.122

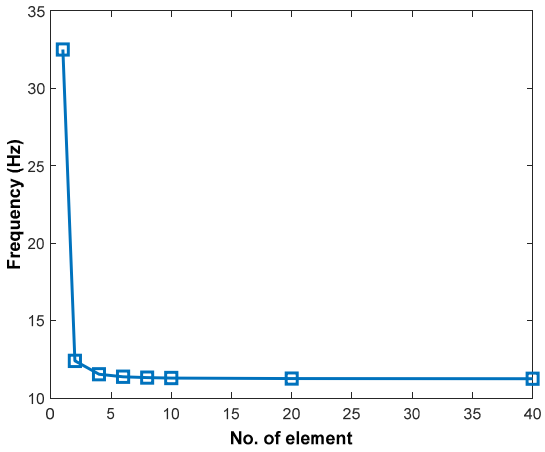

Fig. 10. Convergence rate of natural frequency for mode 3.

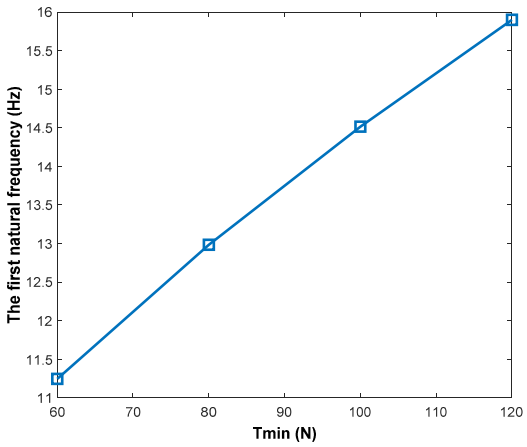

Fig. 11. The dependency of the first natural frequency on T_{min}.

SAP2000 with minimum and maximum errors of 0.74 % and 2.44 %, respectively. Fig. 10 shows the convergence of the proposed finite element algorithm and it is seen that it converges only after six elements. Table 8 shows a comparison of the natural frequency obtained by the FEM algorithm, the modified analytical method and SAP2000. In all three models, each cable element is divided into 40 elements. It is observed that those three methods show almost identical results. Moreover, the minimum and maximum values of mean errors are 0.121 and 0.268, respectively.

Fig. 11 shows the relationship between the fundamental natural frequency of the spatial CDPR on the values of T_{min}.

As shown, when T_{min} increases from 60 N to 120 N, the first natural frequency also increases from 11.245 Hz to 15.901 Hz almost linearly by which dependence of the first natural frequency of the CDPR on the T_{min} is verified. From this observation, it could be inferred that the stiffness of the spatial CDPRs

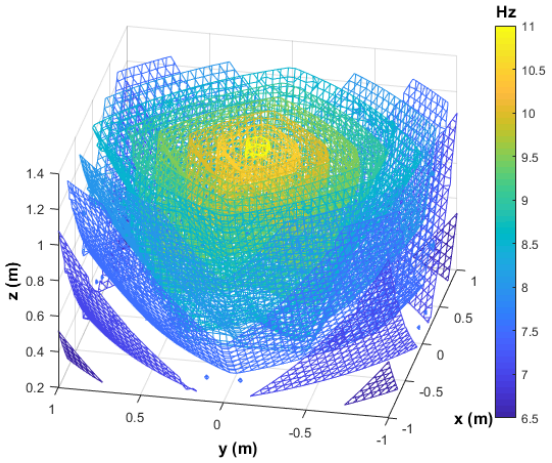

Fig. 12. The first natural frequency of the spatial cable robot in a sub-workspace (-1 m ≤ x ≤ 1 m, -1 m ≤ y ≤ 1 m, 0.25 m ≤ z ≤ 1.25 m) with T_{min} = 60 N.

and the vibration phenomenon can be improved by increasing the value of T_{min} because the stiffness of a structure is related to the natural frequency.

According to Figs. 6 and 11, when the first natural frequency needs to be increased to a specific desired value to improve the stiffness of CDPRs, it could be achieved by altering the values of T_{min}.

Fig. 12 illustrates the first natural frequency of the spatial CDPR in a sub-workspace with T_{min} = 60 N. It is noticed that the first natural frequency of the spatial CDPR increases as the end-effector moves up and reaches the maximum of 10.8 Hz at the top center. This implies that the structural stiffness of the cable structure is low at the low region and is vulnerable to vibration. However, when the end-effector moves towards the top center, the structural stiffness would be high so that it would be vibration resistant.

5. Conclusions

A modified analytical formulation for calculating the stiffness of the cable-driven parallel robot is proposed to model both internal nodes of cables and perfectly vertical cables by dividing cables into numbers of elements and calculating the stiffness matrix of each element without Newton-Raphson iteration. Along with this modified analytical formulation, a new finite element formulation that provides a simple, general and accurate models for vibration analysis is successfully applied to the vibration analysis of CDPRs for the first time.

Both methods were applied to the computation of natural frequencies of the planar and the spatial cable-driven parallel robots for the validation. Both methods yielded the same result with that of the commercial software SAP2000, thereby accuracy and feasibility of the FEM and the modified analytical models are proved in predicting vibration of CDPRs.

From the obtained results in free vibration analysis of CDPRs using the proposed methods, some conclusions can be derived:

1) In the case of the planar cable robot, the structure will have the lowest natural frequency, i.e., the lowest stiffness at the center of the workspace compared to the other poses of the end effector.

2) The spatial CDPR has the highest natural frequency at the top center of the workspace.

3) For all two types of CDPRs, the natural frequencies, i.e., the structural stiffness of the CDPR will be increased by raising the lower boundary of the allowed cable forces.

4) A desired natural frequency to meet some design requirements can be achieved by adjusting the minimum tension in cables.

Acknowledgments

This research was supported by the National Research Foundation of Korea (NRF) grant funded by the Korea government (MSIT) (NRF-2020R1A4A2002855).

References

[1] C. Wright et al., Design of a modular snake robot, *IEEE Int. Conf. Intell. Robot. Syst*. (2007) 2609-2614.

[2] Q. Nguyen et al., Optimized jumping on the MIT cheetah 3 robot, *Proc. IEEE Int. Conf. Robot. Autom.* (2019) 7448-7454.

[3] G. Chen and B. Jin, Position-posture trajectory tracking of a six-legged walking robot, *Int. J. Robot. Autom*., 34 (1) (2019) 24-37.

[4] G. Chen, B. Jin and Y. Chen, Accurate and robust body position trajectory tracking of six-legged walking robots with non-singular terminal sliding mode control method, *Appl. Math. Model*., 77 (2020) 1348-1372.

[5] G. Chen, B. Jin and Y. Chen, Nonsingular fast terminal sliding mode posture control for six-legged walking robots with redundant actuation, *Mechatronics*, 50 (2018) 1-15.

[6] M. A. Khosravi and H. D. Taghirad, Robust PID control of fully-constrained cable driven parallel robots, *Mechatronics*, 24 (2) (2014) 87-97.

[7] X. Diao and O. Ma, Vibration analysis of cable-driven parallel manipulators, *Multibody Syst. Dyn.*, 21 (4) (2009) 347-360.

[8] E. Barnett and C. Gosselin, Large-scale 3D printing with a cable-suspended robot, *Addit. Manuf.*, 7 (2015) 27-44.

[9] E. Ottaviano, Analysis and design of a four-cable-driven parallel manipulator for planar and spatial tasks, *Proc. Inst. Mech. Eng. Part C: J. Mech. Eng. Sci*., 222 (8) (2008) 1583-1592.

[10] S. Nguyen-Van and K. W. Gwak, A novel determination of boundaries of cable forces for cable-driven parallel robots with frequency constraint by using differential evolution algorithm, *ICERA 2019: Advances in Engineering Research and Application* (2019) 35-46.

[11] C. Gosselin, Stiffness mapping for parallel manipulators, *IEEE Trans. Robot. Autom*., 6 (3) (1990) 377-382.

[12] P. Bosscher et al., Cable-suspended robotic contour crafting system, *Autom. Constr*., 17 (1) (2007) 45-55.

[13] D. Q. Nguyen and M. Gouttefarde, Study of reconfigurable suspended cable-driven parallel robots for airplane maintenance, *2014 IEEE/RSJ Int. Conf. Intell. Robot. Syst.* (2014) 1682-1689.

[14] L. Gagliardini et al., Optimal design of cable-driven parallel robots for large industrial structures, *2014 IEEE Int. Conf. Robot. Autom*. (2014) 5744-5749.

[15] G. Abbasnejad, J. Yoon and H. Lee, Optimum kinematic design of a planar cable-driven parallel robot with wrench-closure gait trajectory, *Mech. Mach. Theory*, 99 (2016) 1-18.

[16] S. Behzadipour and A. Khajepour, Stiffness of cable-based parallel manipulators with application to stability analysis, *J. Mech. Des*., 128 (1) (2005) 303-310.

[17] N. G. Dagalakis, J. S. Albus, B.-L. Wang, J. Unger and J. D. Lee, Stiffness study of a parallel link robot crane for shipbuilding applications, *J. Offshore Mech. Arct. Eng*., 111 (3) (1989) 183-193.

[18] S. Kawamura, H. Kino and C. Won, High-speed manipulation by using parallel wire-driven robots, *Robotica*, 18 (1) (2000) 13-21.

[19] H. Yuan et al., Vibration analysis of cable-driven parallel robots based on the dynamic stiffness matrix method, *J. Sound Vib.*, 394 (2017) 527-544.
[20] J. Du et al., Dynamic analysis of cable-driven parallel manipulators with time-varying cable lengths, *Finite Elem. Anal. Des.*, 48 (1) (2012) 1392-1399.
[21] H. D. Do and K. S. Park, Analysis of effective vibration frequency of cable-driven parallel robot using mode tracking and quasi-static method, *Microsyst. Technol.*, 23 (7) (2017) 2577-2585.
[22] M. L. Gambhir and B. de V. Batchelor, A finite element for 3-D prestressed cablenets, *Int. J. Numer. Methods*, 11 (11) (1977) 1699-1718.
[23] M. L. Gambhir and B. de V. Batchelor, Finite element study of the free vibration of 3-D cable networks, *Int. J. Solids Struct.*, 15 (2) (1979) 127-136.
[24] H. B. Jayaraman and W. C. Knudson, A curved element for the analysis of cable structures, *Comput. Struct.*, 14 (3-4) (1981) 325-333.
[25] J. P. Coyette and P. Guisset, Cable network analysis by a nonlinear programming technique, *Eng. Struct.*, 10 (1) (1988) 41-46.
[26] H. T. Thai and S. E. Kim, Nonlinear static and dynamic analysis of cable structures, *Finite Elem. Anal. Des.*, 47 (3) (2011) 237-246.
[27] R. Babaghasabha, M. A. Khosravi and H. D. Taghirad, Robust PID control of fully-constrained cable driven parallel robots, *Mechatronics*, 24 (2) (2014) 87-97.
[28] A. Pott, *Cable-driven Parallel Robots: Theory and Application*, Springer International Publishing (2018).
[29] H. M. Irvine, *Cable Structures*, MIT Press, Cambridge, MA, USA (1981).
[30] H. Yuan, E. Courteille and D. Deblaise, Static and dynamic stiffness analyses of cable-driven parallel robots with non-negligible cable mass and elasticity, *Mech. Mach. Theory*, 85 (2015) 64-81.

Sy Nguyen-Van received his B.S. and M.S. in Mechanical Engineering from Thai Nguyen University of Technology, Thai Nguyen, Vietnam, in 2015, and Sejong University, Seoul, South Korea, in 2019, respectively. He is currently a Lecturer there. His research interests are robotics, evolutionary algorithms, and engineering optimization.

Kwan-Woong Gwak received his B.S. and M.S. in Mechanical Engineering from Korea University, Korea, in 1993 and 1995, respectively, and his Ph.D. with a specialization in nonlinear control system design from the University of Texas, Austin, in 2003. Since 2006, he has been with the Department of Mechanical Engineering, Sejong University, where he is currently a Professor. His research interest includes the robotics, control system design, and mechatronics.